



Middle East Technical University  
Department of Electrical and Electronics  
Engineering

**EE464: Static Power Conversion-II**  
**Term Project Simulation Report**

**By Emine-BOOSTanci**

**Student 1:** Erkin Atay Toka - 2443968

**Student 2:** Erdem Canaz - 2374676

**Student 3:** Canberk Kaçan - 2443240

**Submission Date:** 21.04.2024

**Table of Contents**

Introduction.....3

Topology and Design Selection .....3

Magnetic Design .....7

Preliminary Simulation Results .....18

Component Selection .....24

Future Work .....25

References.....26

## Introduction

This is the simulation report for the hardware project of the EE464 Static Power Conversion II course prepared by Emine BOOSTancı group.

In this project an isolated DC/DC battery charger is designed according to the following specifications.

- Minimum Input Voltage: 20 V
- Maximum Input Voltage: 40 V
- Output Voltage: 12 V
- Output Power: 60 W
- Output Voltage Peak-to-Peak Ripple: 3%
- Line Regulation (Deviation of percent output voltage when input voltage is changed from its minimum to maximum or vice versa): 3%
- Load Regulation (Deviation of percent output voltage when the load current is changed from 10% to 100% or vice versa): 3%

Firstly, possible topologies are introduced to meet these requirements and one of these topologies is chosen. Then, the magnetic design for this topology is presented. Core and copper losses are also discussed. After that, simulation results for the circuit that can be physically realizable is presented. Then the selected components are listed. Lastly, future work is provided in this report.

## Topology and Design Selection

For this project, the following isolated DC/DC converter topologies are assessed.

### Flyback Converter:

Flyback converter topology is suitable for low to medium power applications (typically up to 100 Watts), which fits the 60W requirement.

Advantages:

- Flyback has the minimum number of components. There is only one transformer which is also used as an inductor.
- There is no restriction on the duty cycle.
- Design and control of the topology is the easiest.
- No need for resetting the core's magnetic flux.

Disadvantages:

- Leakage inductance is a problem since it does not have a discharging path. Using snubbers decrease the efficiency of the converter. Adopting a two switch or interleaved topology will complicate the design and control of the converter.
- For high power topologies efficiency is the lowest compared to the other alternatives.

- Output voltage ripple is higher compared to other alternatives. Thus, additional filtering might be needed.

### **Forward Converter:**

The forward converter is suitable for power levels from 50 Watts to a couple of hundred watts.

Advantages:

- This topology is generally more efficient than the flyback converter.
- This topology has better transient response compared to the flyback converter.
- This topology has better lower output ripple compared to the flyback converter due to the output inductor.
- This is the least complex topology after the flyback converter.
- There are no center tapped windings.

Disadvantages:

- This topology has a more complex magnetic design compared to flyback converter due to the additional inductor. Additional inductor will increase the magnetic and copper losses. Notice that the switching frequency seen by the inductor is twice of the switching frequency.
- Flux of the transformer must be reset in one switching cycle. Otherwise, the flux will aggregate and cause saturation which will result in problems in the power transfer. Therefore, the maximum duty cycle is limited. This will complicate the design and control of the converter. This will complicate the design of the converter.
- There are more components compared to the flyback converter thereby it is more expensive and less compact.

### **Push Pull Converter:**

The push pull converter is suitable for medium power levels (100 Watts to a few kilowatts),

Advantages

- Transformer size is reduced because the core is utilized more effectively.
- This topology has better lower output ripple and voltage regulation compared to the flyback and forward converter.
- A smaller variation in  $D$  can help achieve the desired output voltage with twice the gain compared to a forward converter.

Disadvantages:

- Two switches will have to be controlled with a phase shift of half a period. More difficult control. Deadtime adjustment may be required.
- Same problems with additional inductor are present too.

- Inductors' core losses will happen at twice the frequency of operation.
- The duty cycle is also limited for this topology.
- This topology has more components than the flyback and forward converter.
- This topology is more complicated than the other two topologies.

### **Half Bridge and Full Bridge Converter:**

The Half Bridge and Full Bridge Converters are suitable for medium to high power ranges (typically 100 Watts to over 500 Watts).

#### **Advantages**

- Same advantages as push-pull but better efficiency and power density.
- Furthermore, the fill factor challenge eased compared to a push-pull converter since there is a single primary.

#### **Disadvantages**

- Same disadvantages as push-pull but complexity of the converter is increased.
- For full bridge converter additional switches increase the losses.
- For half bridge converter nonidentical switches might cause problems in terms of voltage division.

Push-pull, half and full bridge converter topologies are overdesign for this project since the output power is 60W. Therefore, the real candidates are flyback and forward converter topologies. Since there is a limit on the duty cycle and risk of flux accumulation on the core, the design and control of the forward converter. Also, additional inductance and 3<sup>rd</sup> winding increase the complexity of the magnetic design. Although the flyback converter's efficiency is inferior due to the snubber circuit for leakage inductance discharge, an optimization or an application note can be utilized to optimize the efficiency of the converter. Moreover, two switch flyback topology can be used. Although this will increase the complexity due to the drive of the high side switch it will enable us to feed the stored energy on the leakage inductor back to the input capacitor instead of dissipating it on the resistor in the snubber circuit. This will increase efficiency. Another disadvantage of the two switch flyback is the fact that the duty cycle is limited to 0.5 due to the diodes on the input side. For now, the snubber design will be selected as the solution of the discharge path of the leakage inductor. It is aimed to complete the first design as soon as possible so that the design can be changed to two switched flyback is efficiency would be smaller than the aimed one.

Another important decision is whether to operate at CCM or DCM. Since flux drops zero at DCM of operation the magnetic core is utilized better. Also, control of the converter is easier due to the linear relationship between output voltage and duty cycle as can be seen in Figure 1. However, the analytical understanding of the DCM operation is harder in terms of equations therefore the design is more complex. In addition to this, the current ripple is higher for DCM operation. This will increase semiconductor losses. Furthermore, the output voltage ripple will increase, and an

additional filter might be used to meet the 3% voltage ripple condition. Since a controller that can operate at CCM is found, to meet voltage ripple and load regulation criteria CCM operation is chosen.

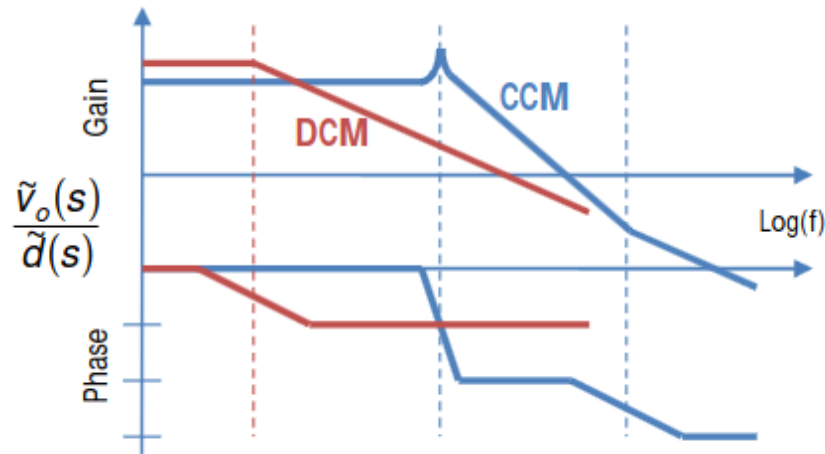


Figure 1 Bode Plots For DCM and CCM Mode of Operation

After selecting the topology and the mode of operation, switching frequency, turns ratio and duty cycle range are determined.

- **Switching frequency ( $f_s$ ) selection:** Switching frequency is chosen as 90 kHz. Increasing the switching frequency will enable us to have a smaller ripple at the output and give us the chance to decrease  $L_m$ . Decreasing  $L_m$  will enable us to utilize the core more efficiently. However, increasing frequency will increase the switching losses of the transistors, core losses and conduction losses. In addition to these, increase in switching frequency will increase the leakage inductances. Therefore, an optimal choice is made as 90 kHz. Also, it is aimed to complete the project in PCB which will solve the leakage inductance problem compared to Pertinax.
- **Turns Ratio (N) and Duty Cycle Range (D) Selection:** Since the overall design can be changed to two switched flyback according to the resulting efficiency, a design that is compatible with both topologies should be adopted. That indicates the duty cycle should not exceed 0.5. Exceeding 0.5 will introduce DCM operation due to the diode clamp in the two switched flyback. Also, choosing an analog controller with the maximum duty cycle of 0.5 is logical so that the converter never falls into an open loop. Hence, duty cycle close and higher than 0.5 is avoided. The voltage relationship for the flyback topology is given below. According to this equation, the maximum and minimum duty cycle for different turns ratio is plotted in Figure 2. The turns ratio is selected as 1 since the understanding will be much easier and the maximum and minimum duty cycles are computed as 0.375 and 0.23 which are smaller than 0.5.

$$\frac{V_{out}}{V_{in}} = N \frac{D}{(1 - D)}$$

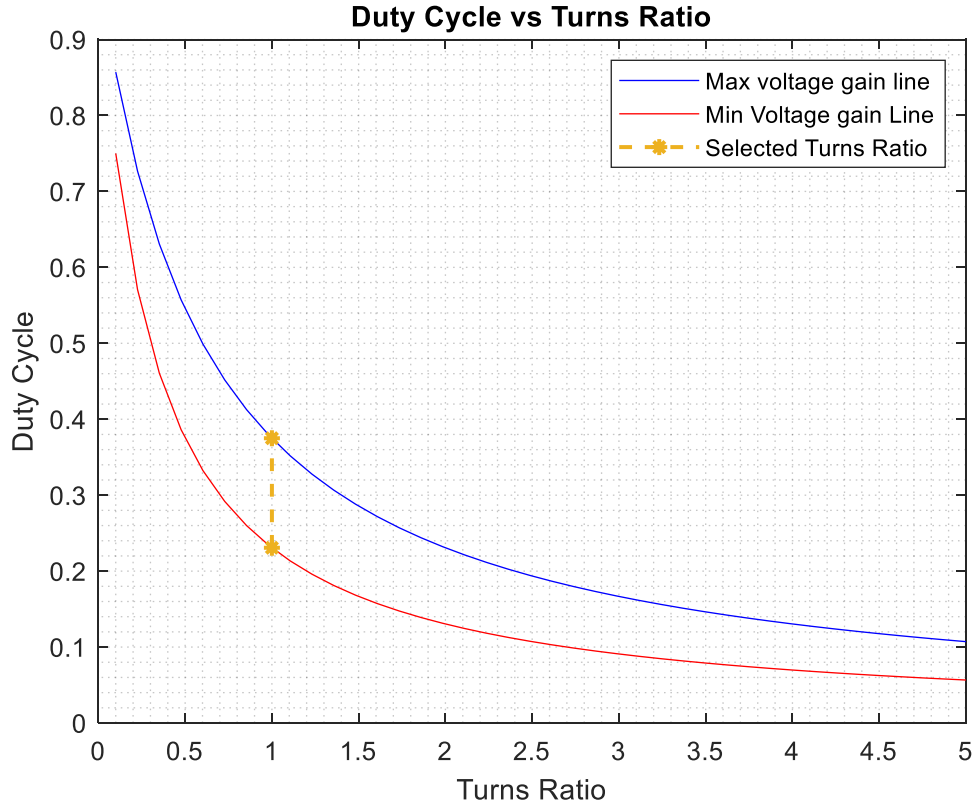


Figure 2 Duty Cycle vs Turns Ratio wrt Max and Min Voltage Gain

## Magnetic Design

In this part, we need to decide the magnetizing inductance on the primary side  $L_m$ , a magnetic core, number of turns and the winding cables. Then, the magnetic and copper losses of the transformer are calculated. Lastly, the transformer is wound and magnetizing and leakage inductances and primary and secondary winding resistances are measured by LCR meter.

Before selecting the core, the magnetizing inductance in the primary side  $L_m$  is determined. The  $L_m$  decided so that the converter does not work in DCM mode but also the peak inductor current is not too high so that the core is not saturated. For these conditions the average inductor current and the current ripple are important. The average inductor current depends on the average current and duty cycle. To find the average input current the efficiency of the converter must be known. For now, the efficiency of the converter will be estimated as 80%.

$$P_{in} = \frac{P_{out}}{\eta} = 75 \text{ W}$$

$$I_{in,avg,max} = \frac{P_{in}}{V_{in,min}} = 3.75 \text{ A}$$

$$I_{in,avg,min} = \frac{P_{in}}{V_{in,max}} = 1.875 \text{ A}$$

Input current is equal to the primary side inductor current for  $DT_s$  and zero for the rest of the switching period. The relationship between the primary side inductor current and the input current is given as follows.

$$I_{Lm,avg} = \frac{I_{in,avg}}{D}$$

Maximum and minimum average primary side inductor current is calculated as 10 A and 8.125 A respectively.

For the current ripple  $K_{RF}$  is defined as the ripple factor as given in Figure 3.

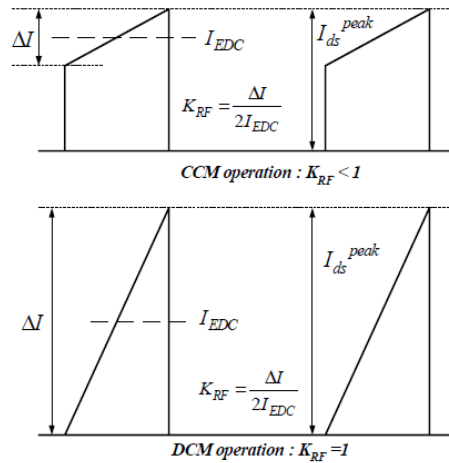


Figure 3 Ripple Factor

In order to avoid DCM operation  $K_{RF}$  must be smaller than 1. Also, smaller  $K_{RF}$  will decrease the output voltage ripple. However, lower  $K_{RF}$  might increase the transformer flux which will lead to the saturation of the core. For safety 0.7  $K_{RF}$  is avoided. The needed inductance can be calculated as follows.

$$L_m > \frac{(V_{in}^{max} D_{min})^2}{2 P_{in} f_s K_{RF}} = \frac{(40V \cdot 0.238)^2}{2 (75W)(90kHz)0.7} = 9.6 \mu H$$

Primary side inductance is selected as 20  $\mu H$ .

The saturation must be avoided to transfer power efficiently. The saturation is determined by the peak current. The primary peak current is plotted with respect to the input voltage in Figure 4.



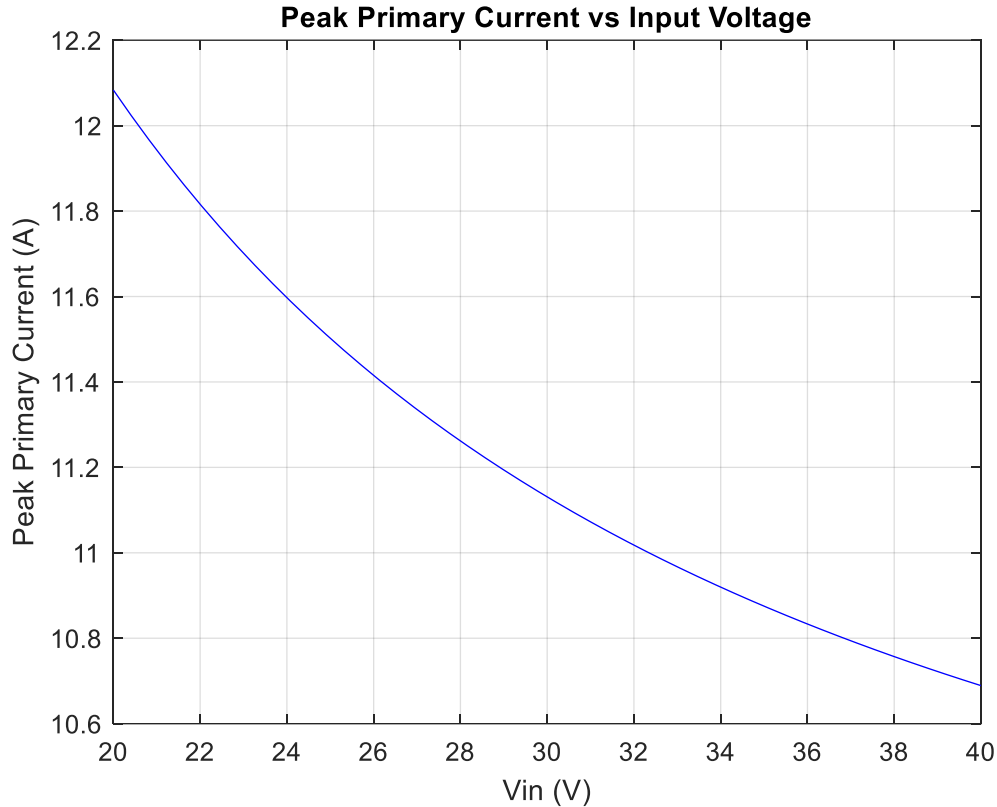


*Figure 4 Peak Primary Current vs Input Voltage*

From Figure 4 it can be seen that the maximum peak current occurs when the input voltage is minimum. This value is calculated as 12.1 A.

Now it is time for magnetic core selection. For core selection there are two options, a distributed gap core or a ferrite core. The relative permeability of the distributed gap cores is small, the leakage inductance is higher with respect to the ferrite core. Since the leakage inductance is dangerous for the switches a ferrite core 0R45530EC which is available in the laboratory is selected. One of the reasons to select this core is that its cross section area is high thus the saturation of the core can be easily avoided. Also, operating around 100 mT is aimed so that the core losses will be minimized although the volume of the core is increased. Another reason for selecting this core is the fact that its window area is the largest. This will ease the winding procedure. In addition to the primary and secondary windings, we will utilize the auxiliary winding to power up the controller.

To decide the number of turns in the primary side the core flux density and the length of the air gap will be considered. Half of the flux passing through the center leg of the core will be passing through the side legs. Nevertheless, the cross section area of the side legs is not exactly half of the cross section area of the center leg. Therefore, the magnetic field density will not be equal in the center leg and the side legs. It is known that the maximum primary current will occur when the duty cycle is maximum. Thus, the maximum magnetic field density will occur in the maximum duty cycle. The relationship between primary turns number and magnetic field density is given below.

$$R_{core} = \frac{N_1^2}{L_m}$$

$$\phi = \frac{N_1 I_{Lm,peak}}{R_{core}} = \frac{L_m I_{Lm,peak}}{N_1}$$

$$B = \frac{\phi}{A} = \frac{L_m I_{Lm,peak}}{A N_1}$$

To illustrate the relation between magnetic flux density and primary turns number these two are plotted with respect to each other in Figure 5. It can be seen that the center leg saturates more than the side legs.

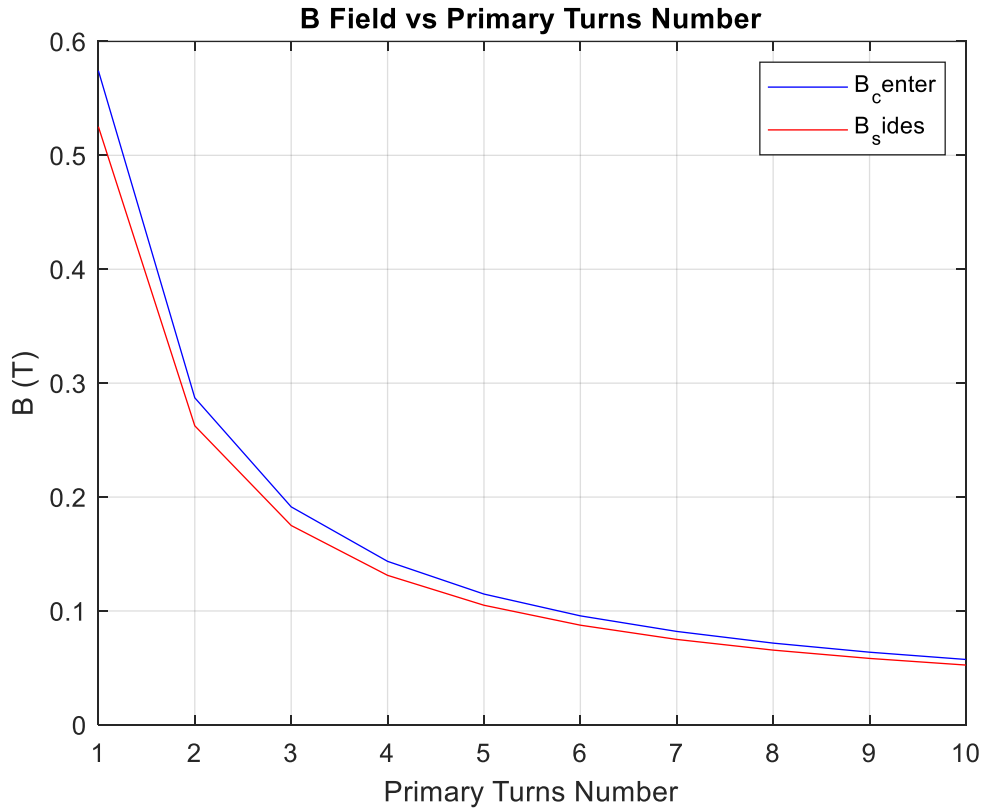


Figure 5 Magnetic Field Density vs Primary Turns Number

Before selecting the primary turns number, we need to also consider the air gap length. Since the relative permeability of the core is 2300 the reluctance of the core is negligible with respect to air gap reluctance. The magnetic circuit of the transformer is given in Figure 6. Reluctance of the side legs and center leg can be found as follows.

$$R_{side} = \frac{l_{gap}}{\mu_0 A_{side}}$$

$$R_{center} = \frac{l_{gap}}{\mu_0 A_{center}}$$

$$R_{core} = R_{center} + \frac{R_{side}}{2} = \frac{N_1^2}{L_m}$$

$$l_{gap} = \frac{N_1^2}{L_m} \frac{2\mu_0 A_{center} A_{side}}{A_{center} + 2A_{side}}$$

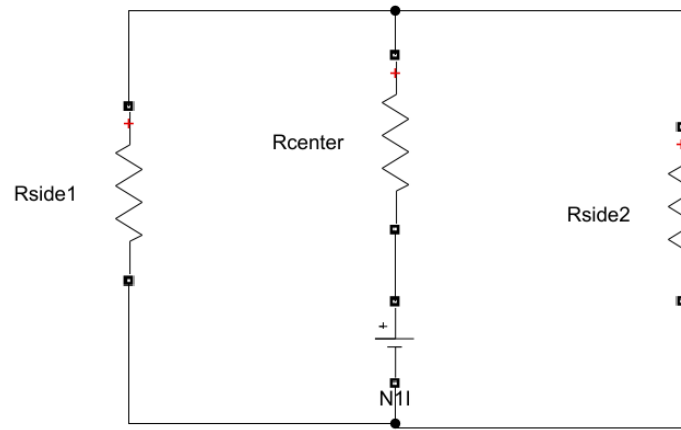


*Figure 6 Magnetic Circuit of the Transformer*

In order to determine the primary turns number, the air gap length is plotted with respect to the primary turns number in Figure 7.

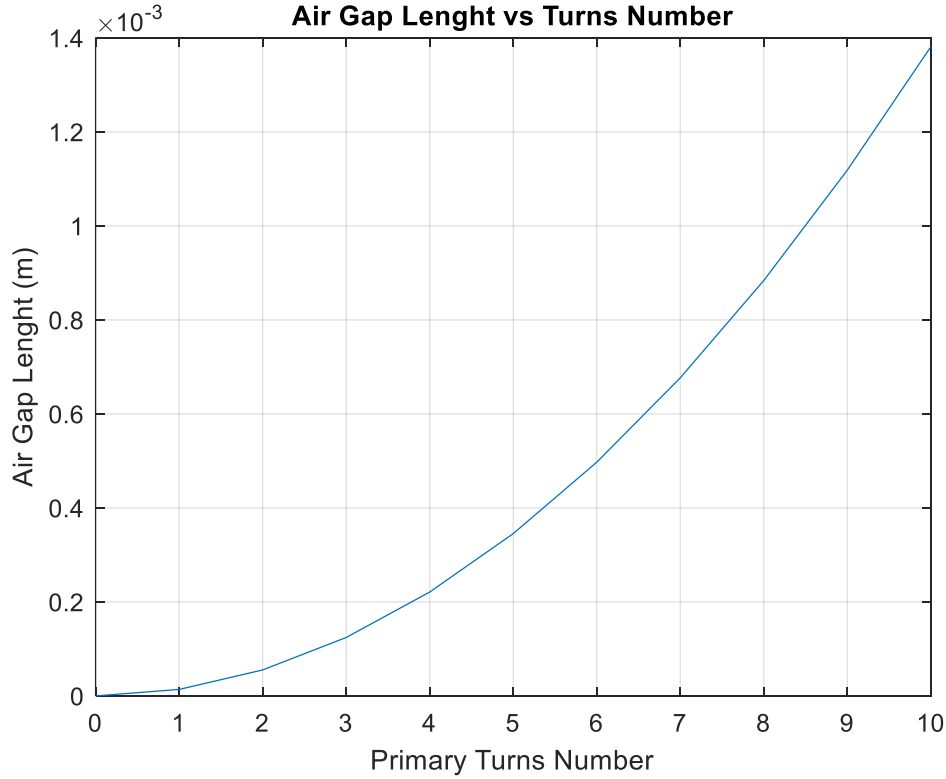


*Figure 7 Air Gap Length vs Primary Turns Number*

From Figure 5 it can be seen that increasing the primary turns number will decrease the magnetic field density. However, increasing the primary turns number will also increase the air gap length. This is not desired due to the increasing fringing fields with increasing airgap length which can be seen from Figure 7. From both of these figures, the primary turns number is selected as 7. It can be seen that maximum magnetic flux density of the center leg is 82 mT and air gap length is 7 mm for the selected turns number. The peak magnetic flux density is small enough to minimize the core loss and also the air gap length is small enough to ignore the fringing fields.

$$N_1 = 7 \text{ turns}$$

$$N_2 = \frac{N_2}{N_1} N_1 = 1 * 7 = 7 \text{ turns}$$

Magnetic field density vs the duty cycle for center and side legs are given in Figure 8.

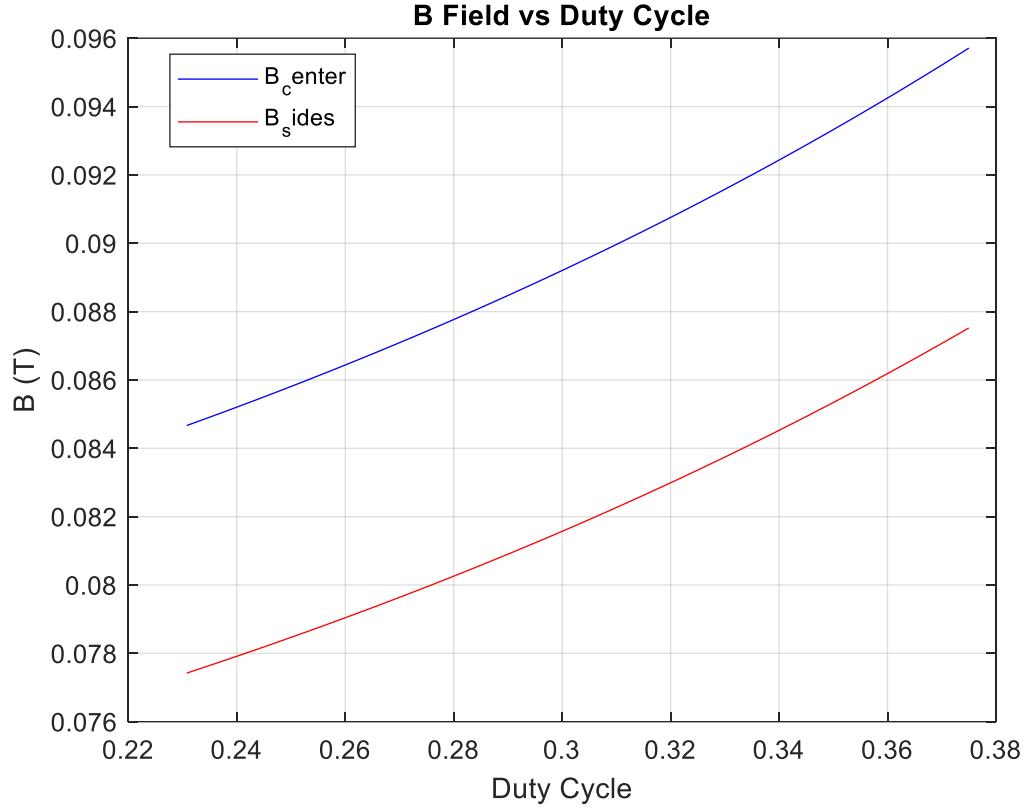


Figure 8 Field vs Duty Cycle

Now we need to choose an AWG cable for primary and secondary. First, the skin depth is calculated for the switching frequency which is 90 kHz.

$$\delta = \sqrt{\frac{\rho_{Cu}}{\mu_0 \pi f_s}} = \sqrt{\frac{1.724 \cdot 10^{-8}}{\mu_0 \pi 90 \cdot 10^3}} = 0.22 \text{ mm}$$

$$A_{strand} = \pi \delta^2 = 0.1524 \text{ mm}^2$$

The copper area must be equal or smaller than the strand area. Hence, AWG26 with  $0.129 \text{ mm}^2$  is selected as primary and secondary cable.

Now we need to find how many cables to parallel in order to carry primary and secondary currents. Thereby, the rms value of the primary and the secondary currents are calculated. RMS value for an inductor current given in Figure 9 can be calculated as follows.

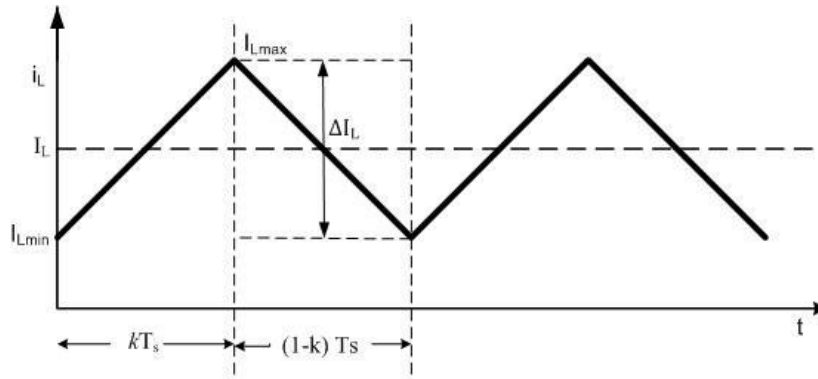


Figure 9 Typical Inductor Current

$$I_{L,rms} = \sqrt{I_L^2 + \frac{\Delta I_L^2}{12}}$$

According to this formulation rms primary current vs input voltage is plotted in Figure 10. From Figure 10 it can be seen that the rms primary and secondary currents reach their maximum value of 10 A at minimum input voltage.

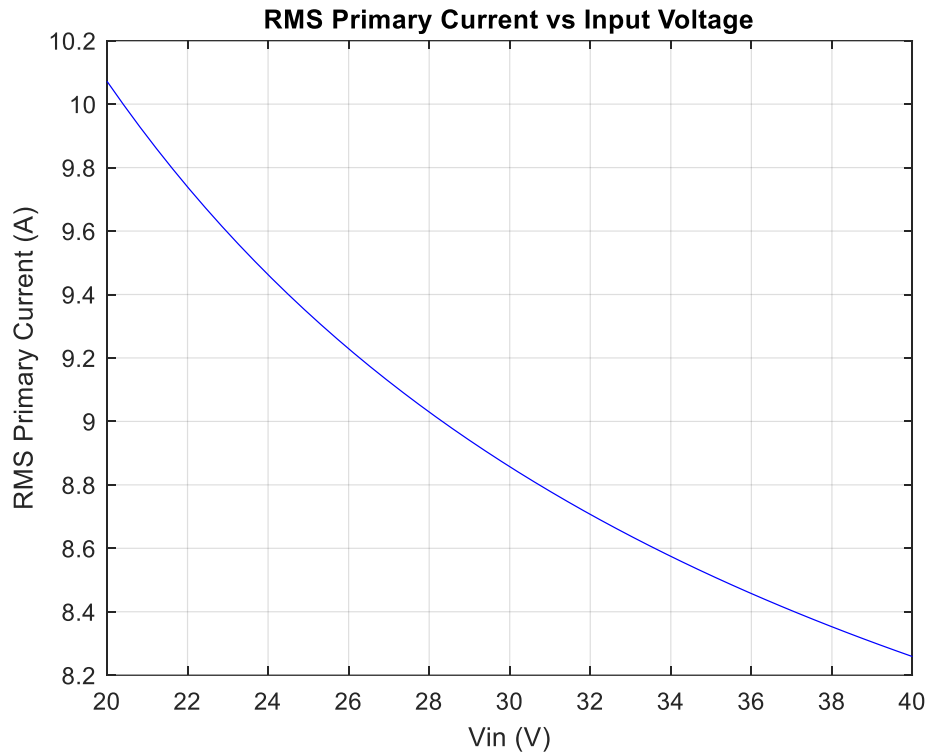


Figure 10 RMS Primary Current vs Input Voltage

The current carrying capacity of the AWG26 cable is 0.361 A. However, this value is indicated for a straight line. Since we will wound the cable, the capacity will drop. To take the wounding effect

into account, the current carrying capacity will be multiplied by 0.75. The number of parallel cables can be found as follows.

$$\#parallel\ cables = nearest\ integer\left(\frac{I_{rms\ max}}{0.75\ Current\ carrying\ capacity_{AWG26}}\right)$$

For primary and secondary the number of parallel cables is calculated as 35. The area of an AWG26 cable is  $0.129\ mm^2$ . Total cable area can be calculated as follows.

$$A_{Cable} = A_{AWG26}(N_1\ \#primary\ parallel\ cables + N_2\ \#secondary\ parallel\ cables)$$

$$A_{Cable} = 63.21\ mm^2$$

The window area of the core is calculated from its dimensions as  $375\ mm^2$ .

$$Fill\ Factor = \frac{A_{Cable}}{A_{window}} = 0.1683$$

The fill factor is acceptable up to 0.3 to 0.4. Although our choice might seem like an overdesign, we plan to utilize auxiliary winding to power up the controller. In addition to this increasing the fill factor will complicate the winding process. Thereby, the leakage inductance might be increased due to a poor winding process.

Since the radius of the conductor is chosen smaller than the skin depth both AC resistance is quite the same as the DC resistance. This is verified by a website that measures the AC resistance of a specified cable [1]. The mean length turn of the core is calculated from the geometry in order to find the length of the wounded cable. Also, a safety factor of 1.5 is taken due to the cable thickness. This mean length turn is multiplied by the turns number to find the total length of the cables.

$$R_{primary} = \rho \frac{l}{A} = 1.678\ 10^{-8}\Omega m \frac{1.0219\ m}{35\ \pi \left(\frac{0.439\ 10^{-3}}{2}m\right)^2} = 3.9\ m\Omega$$

$$R_{secondary} = R_{primary} = 3.9\ m\Omega$$

Maximum copper losses can be calculated from the maximum rms current which is found as 10 A for primary and secondary.

$$P_{copper,primary} = I_{primary\ rms}^2 R_{primary} = 0.3965\ W$$

$$P_{copper,secondary} = I_{secondary\ rms}^2 R_{secondary} = 0.3965\ W$$

$$P_{copper} = P_{copper,primary} + P_{copper,secondary} = 0.793\ W$$

For core losses an excel file is obtained for ferrite materials from [2]. In this Excel file, Steinmetz coefficients are available. Steinmetz equation and coefficients for the R type material are given below.

$$P_{CL} = \frac{a f^x B^y L(T)}{100} \text{ mW/cm}^3$$

$$L(T) = b - cT + dT^2$$

Material	Frequency Range	a	x	y	b	c	d	Core Loss $P_{CL}$ (mW/cm <sup>3</sup> )
R Material	20kHz-150kHz	3.53	1.420	2.880	1.970000000	0.022260000	0.0001250000	30.89
	150kHz-400kHz	5.88E-04	2.120	2.700	2.160000000	0.023270000	0.0001170000	

Figure 11 Steinmetz Coefficients for R Material

For maximum core loss, the maximum flux density which is 0.82 mT has been chosen. For operating temperature and frequency, 60°C and 90kHz are chosen respectively. Core loss density is calculated as 30.89 mW/cm<sup>3</sup> for this operation condition. To find the core loss the core loss density is multiplied by twice the volume of the core (volume of the core is 208 cm<sup>3</sup>). Since two EC cores are used. Total core loss is found to be 3.21 W. Core loss is approximately 4 times higher than the copper loss. Since we operate at high frequencies this is expected. In order to use in unideal modelling of the converter  $R_{core}$  can be found as follows.

$$R_{core} = \frac{V_{out}^2}{P_{core}} \left( \frac{N_1}{N_2} \right)^2 = 498 \Omega$$

After wounding the transformer LCR meter is used to calculate the leakage and magnetizing inductance. Since the LCR meter is not reliable for resistance calculations, to calculate the resistance windings are connected to the power supply and the maximum current is set to 5A. Then the voltage across the windings is measured by the multimeter and resistance is calculated from the Ohms Law. Supplied voltage is not used since the resistance of the cables that are used to connect the power supply and transformer is comparable with the winding resistance. For both windings voltage is measured as 0.023 V when 5A is supplied by the DC power supply. This means the resistance of the primary and secondary windings is 4.6 mΩ which is close to our calculations.

To understand the logic of the measurement technique of the leakage and magnetizing inductance equivalent model of the transformer given in Figure 12 is investigated. First, the secondary side is left open circuited. The measurement gives us the sum of primary leakage inductance and magnetizing inductance. Nevertheless, the measurement can be taken as magnetizing inductance since leakage inductance is much smaller than the magnetizing inductance. Magnetizing inductance is measured as 20.94 μH. For leakage inductance calculation, the secondary is kept short circuited, and inductance is measured. This measurement corresponds to primary leakage inductance plus secondary leakage paralleled magnetizing inductance. Since leakage inductance is much smaller than the magnetizing inductance, secondary leakage paralleled magnetizing inductance can be



approximated as secondary leakage inductance. Thus, measured inductance  $0.42 \mu\text{H}$  is the sum of primary and secondary leakage inductances. Since the turns ratio is 1, we can assume that leakage inductances are equal. This will yield primary and secondary leakage to be  $0.21 \mu\text{H}$ . Measurements for open and short circuited secondary are given in Figure 13 and 14 respectively.

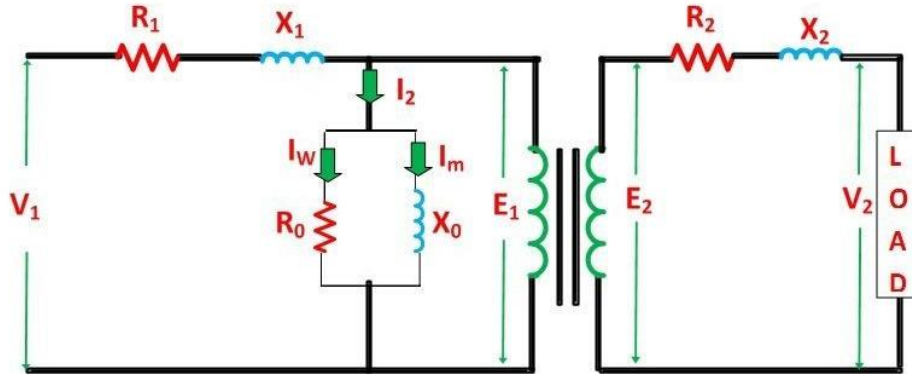


Figure 12 Equivalent Circuit of the Transformer

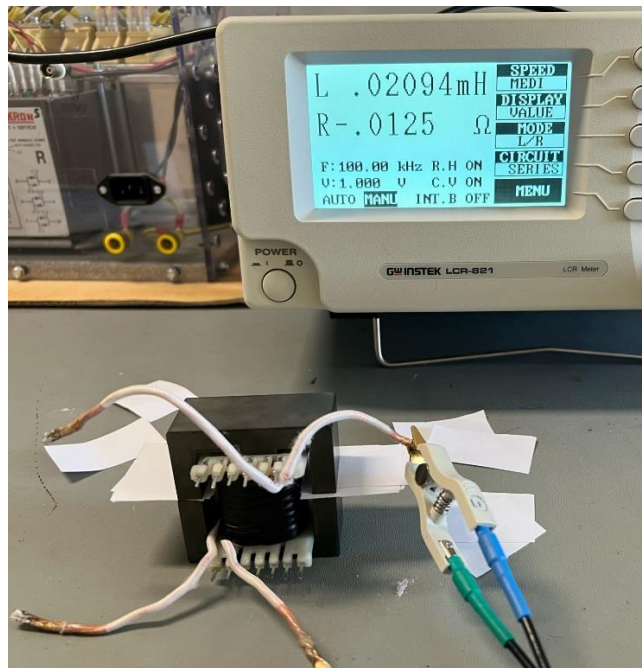


Figure 13 Open Circuit Measurements

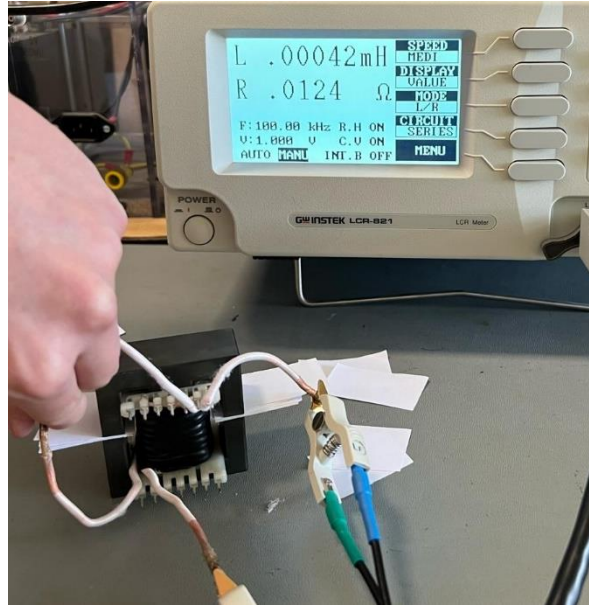


Figure 14 Short Circuit Measurements

## Preliminary Simulation Results

Our circuit can be separated to 11 different sections according to their purposes. Those sections are listed below with their brief explanations

- **Input Filter:** Responsible for smoothing the input current and ensuring a stable input voltage for the circuit.
- **Auxiliary Power Supply:** Responsible for powering the controller IC.
- **Leakage snubber:** Responsible for eliminating the voltage spikes at the mosfet drain due to leakage inductance.
- **Flyback Transformer:** Main power transfer element.
- **Output Diode Snubber:** Reduces reverse voltage stress on the output diode.
- **Output Filter:** Responsible for smothing the output current and minimizing the output voltage ripple.
- **Indicator Leds:** It serves two purposes. First, it indicates whether the output is connected to a battery or regulated by the IC. Second, it shows that the battery is fully charged and now in constant voltage charging mode.
- **Feedback Circuit:** It transfers the output voltage information to IC in an isolated manner.
- **Controller IC:** It controls the switch in a closed-loop manner.
- **Current Sensor:** It measures the drain current of the mosfet with hall effect sensor.
- **Mosfet:** The main switching element.

The detailed simulation used in this results is archived on [Github](#), and its zoom-out view is given in Fig.15. Zoomed-in view of the circuit models for each section are also provided below.



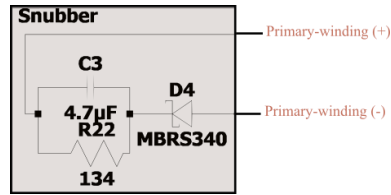


Figure 18 Zoom-in view of the leakage snubber

## Flyback Transformer:

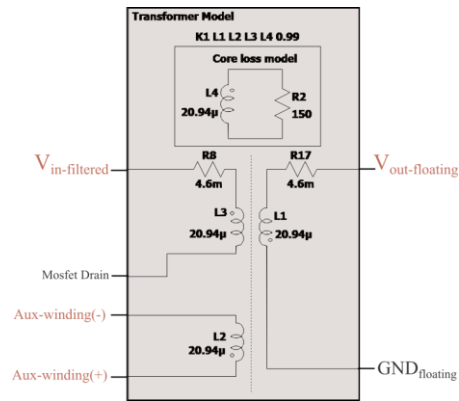


Figure 19 Zoom-in view of the flyback transformer

## Output Diode Snubber:

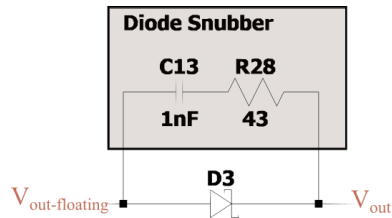


Figure 20 Zoom-in view of output diode snubber

## Output Filter:

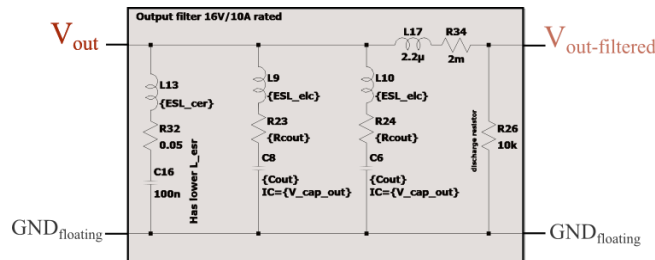


Figure 21 Zoom-in view of the output filter

## Indicator Leds:

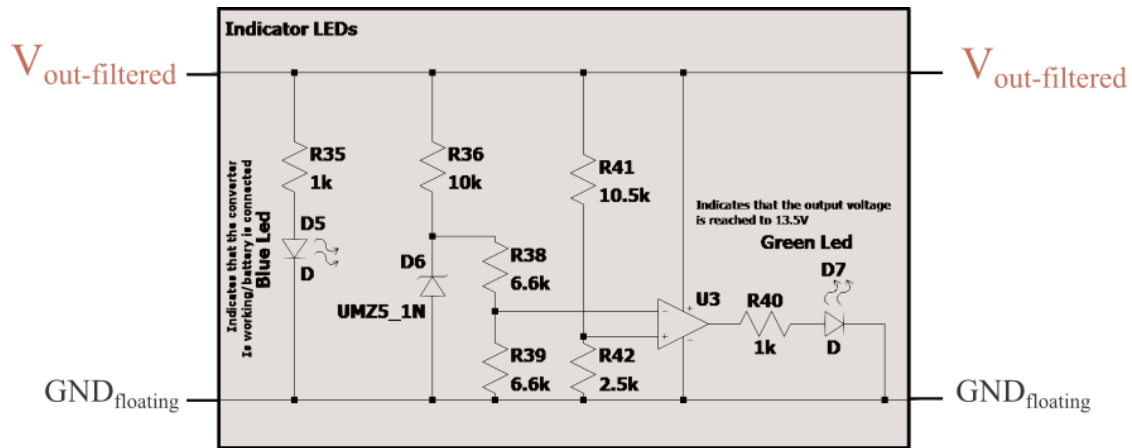


Figure 22 Zoom-in view of the indicator leds

### Feedback Circuit:

The optocoupler in the model functions as a current mirror. Here, the current flowing through the optocoupler is multiplied by the Current Transfer Ratio (CTR) and then fed into the base of an NPN bipolar junction transistor (BJT). The mirrored current is further multiplied by the BJT's beta value. This approach allows for controlled adjustment of the collector current. The circuit is configured such that feedback voltage is 2.5V when the output voltage is 13.5V.

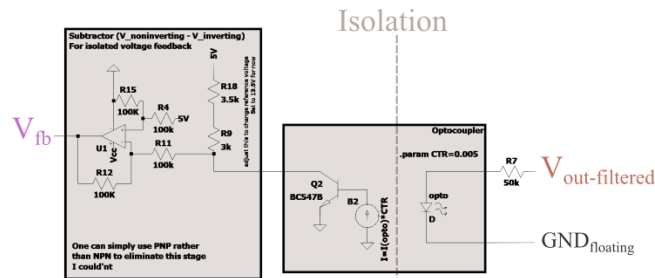


Figure 23 Zoom-in view of the feedback-circuit

### Controller IC:

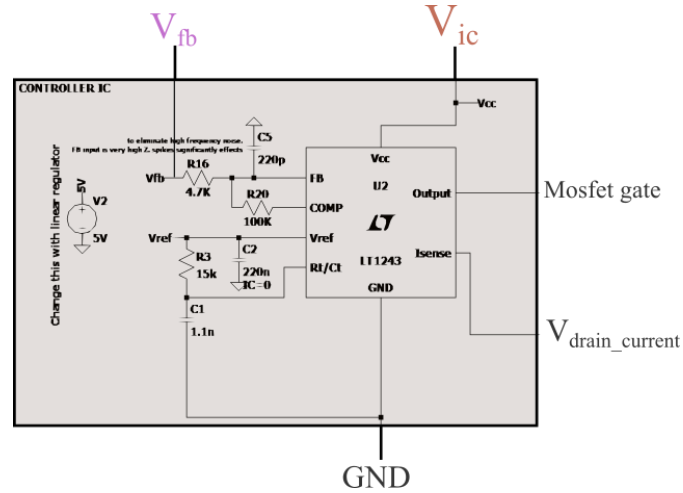


Figure 24 Zoom-in view of controller IC

### Current sensor:

As current sensor, ACS712-30A IC is modelled. Its output voltage is determined by the current passing through two of its terminals. The output voltage is given by the following formula

$$V_{\text{drain\_current}} = 2.5 + 0.083 \cdot I_{\text{drain\_current}}$$

Due to voltage divider, when the the allowed peak current is reached, the output of the block is 1V.

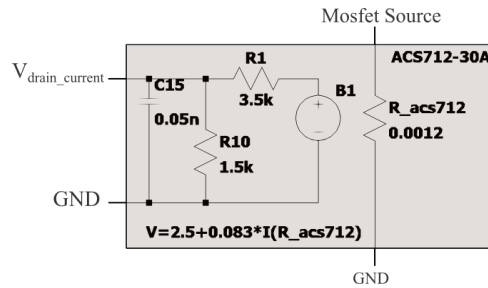


Figure 25 Zoom-in view of the current sensor

### MOSFET:

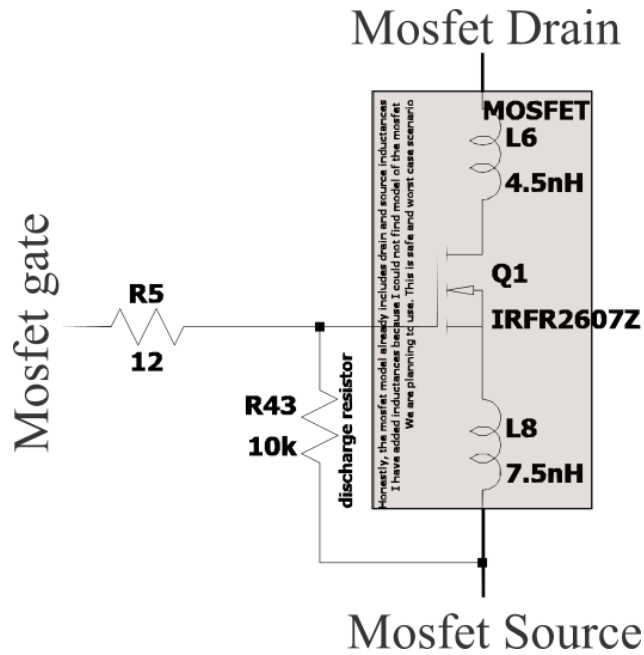


Figure 26 Zoom-in view of the MOSFET

### Simulation results:

The simulation was conducted using input voltages of 20, 25, 30, 35, and 40 volts, along with battery voltages of 11, 12, and 13 volts. The results show that our circuit achieves an efficiency of approximately 75-80% when implemented practically. The distribution of the input power averaging all results is shown in Fig 27. Detailed simulation results are shown in the Fig. 28.

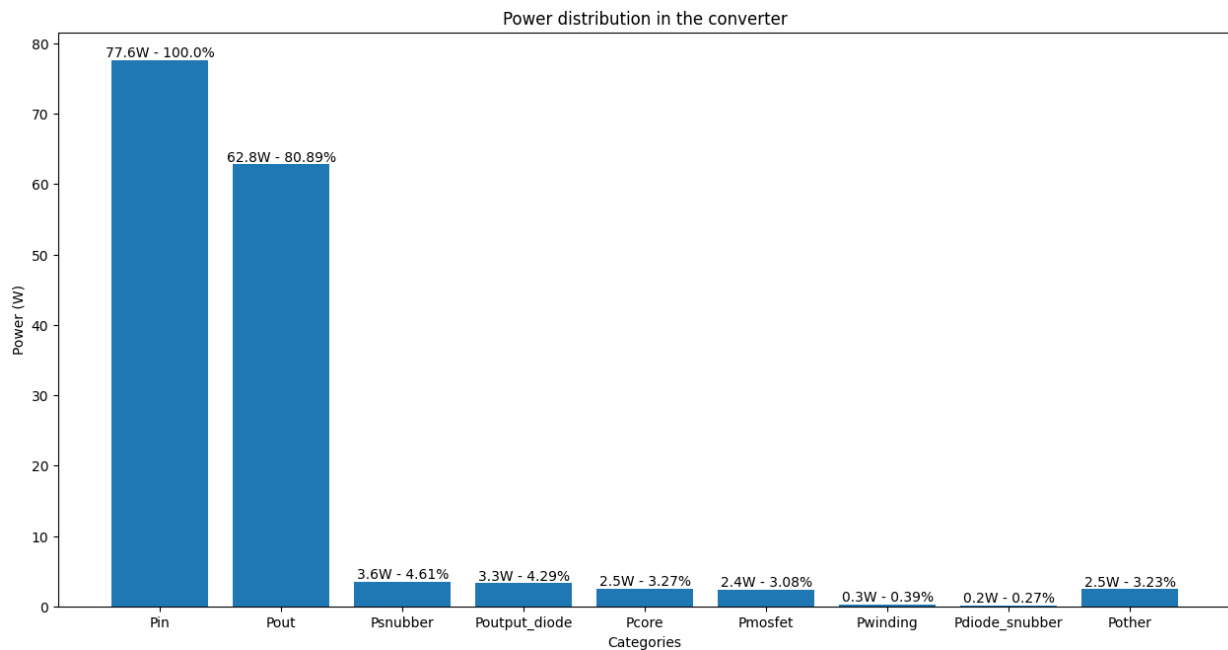


Figure 27 Power distribution in the converter

Vin (V)	Vbat (V)	efficiency (%)	Duty	Iin-mean (A)	Iin-ripple(A)	Ibat (A)	Ibat_ripple (A)	Pin (W)	Pout (W)	Psnubber (W)	Pdiode_snubber (W)	Pmosfet (W)	Poutput_diode (W)	Pcore (W)	Pwinding (W)	Vsnubber_diode (V)	Vds (V)	VoutRipple (V)
20	11	80	0,40	3,44	0,40	4,86	0,37	68,20	54,76	3,46	0,10	2,13	3,22	1,55	0,33	45,00	45,00	0,02
20	12	81	0,40	3,57	0,41	4,65	0,37	70,72	57,14	3,70	0,10	2,15	3,10	1,68	0,30	45,00	45,00	0,05
20	13	81	0,40	3,59	0,40	4,33	0,36	71,12	57,46	3,80	0,10	2,08	2,83	1,80	0,30	45,00	45,00	0,05
25	11	81	0,35	2,94	0,37	5,24	0,35	73,14	59,15	3,34	0,10	2,26	3,45	1,95	0,30	50,00	50,00	0,06
25	12	81	0,35	3,05	0,38	5,01	0,35	75,99	61,70	3,70	0,13	2,30	3,30	2,14	0,30	50,00	50,00	0,06
25	13	81	0,35	3,07	0,37	4,67	0,34	76,40	62,00	3,80	0,14	2,20	3,00	2,30	0,30	50,00	50,00	0,08
30	11	81	0,32	2,58	0,35	5,51	0,33	77,02	62,29	3,50	0,16	2,41	3,63	2,35	0,30	55,00	57,00	0,10
30	12	81	0,32	2,68	0,37	5,29	0,33	80,16	65,10	3,65	0,17	2,44	3,46	2,54	0,30	55,00	57,00	0,10
30	13	82	0,32	2,61	0,35	4,77	0,31	78,00	63,69	3,65	0,18	2,25	3,00	2,71	0,30	55,00	57,00	0,10
35	11	81	0,27	2,23	0,33	5,73	0,30	80,26	64,76	3,40	0,20	2,59	3,76	2,75	0,30	60,00	60,00	0,10
35	12	81	0,27	2,40	0,33	5,50	0,30	83,62	67,76	3,54	0,20	2,62	3,60	2,98	0,30	60,00	60,00	0,10
35	13	81	0,27	2,28	0,30	4,83	0,30	79,11	64,35	3,60	0,22	2,32	3,00	3,19	0,30	60,00	60,00	0,10
40	11	80	0,23	2,08	0,30	5,90	0,28	83,11	66,75	3,40	0,24	2,77	3,86	3,14	0,30	65,00	65,00	0,10
40	12	81	0,23	2,17	0,30	5,67	0,28	86,64	69,90	3,64	0,26	2,89	3,70	3,40	0,30	65,00	65,00	0,10
40	13	81	0,23	2,02	0,29	4,88	0,26	80,67	64,94	3,50	0,27	2,42	3,08	3,64	0,30	65,00	65,00	0,10

Figure 28 Detailed simulation results

## Component Selection

According to the waveforms, shown in the Simulation part, we have decided on the important components. The core selection was justified in the Magnetic Design part; thus, there will not be any information about the magnetic core in this section.

- **MOSFET:** IRFU3710ZPbF [3]

As shown in the Simulation section, the MOSFET has a peak voltage level of around 70V, due to ringing, which means the MOSFET should endure a voltage stress much higher than the input voltage. Moreover, this value is changing according to the designed snubber which is not finalized in this project for the time being. To account for all of this, a relatively high safety margin must be considered while choosing a MOSFET. IRFU3710ZPbF can bear 100V and 39A while having an 18mΩ which is quite good for our design; thus, we have chosen this MOSFET.

- **IC:** UC3845AN [4]



UC3845AN is a current-mode PWM controller. It has a low start-up current ( $< 0.5 \text{ mA}$ ), which is advantageous for the flyback converter. It can operate up to  $500\text{kHz}$  and can provide up to a %50 duty cycle. Moreover, it is selected since its usage in isolated power converters is highly known and a high number of sources can be found on its driving circuitry.

- **Diode:** DSA30C100PB [5]

While the design includes 4 diodes, three Schottky and one Zener, the most important ones are the one at the secondary winding side and the one at the snubber. The snubber diode has a peak voltage of  $70\text{V}$ , just like the MOSFET. However, it has a lower forward current than the MOSFET with a  $7\text{A}$  peak. The chosen diode can withstand  $100\text{V}$  and it has an  $I_F$  rating of  $15\text{A}$ . The voltage drop in the conduction is  $0.73\text{V}$  which is one of the lowest values we could find; thus, we have chosen this diode since efficiency is one of the main concerns in this project. Also, since both diodes have similar waveforms, we will be using this for both of the diodes.

- **Optocoupler:** LTV-816 [6]

We have chosen a single-channel optocoupler since we need only one channel and cost can increase with the increasing number of channels. Moreover, we have chosen this optocoupler since it is easy to find and economically feasible.

- **Output Capacitor:** PKLH-016V471MG125 [7]

We have chosen this one as the output capacitor. It is an Aluminum Electrolytic Capacitor with a voltage rating of  $16\text{V}$ . While only one of them is  $470\mu\text{F}$ , we will parallel four of them to reduce ESR while having the wanted capacitance rating at the output side.

Aside from the components mentioned above, various resistors and capacitors will be used.

## Future Work

The project is under development; therefore, the design decisions may change. While we believe that the magnetic design and transformer realization parts were finished, there are several parts that need to be improved. In the future, we will improve the snubber circuit and tune the  $R_{sn}$  and  $C_{sn}$ . An optocoupler circuitry will be implemented. Moreover, an output filter will be designed. We plan to progress quickly to the implementation part to keep improving the converter throughout the project. If everything goes according to the plan, we are planning to implement the circuit on a PCB and make a case. The efficiency will be our number one priority, as mentioned above. Moreover, the design will be revised, if needed, after the feedback session.

## References

- [1] W. (n.d.). Round Wire ac Resistance Calculator. <https://chemandy.com/calculators/round-wire-ac-resistance-calculator.htm>
- [2]“Magnetics - Ferrite Core Loss Calculator.” <https://www.mag-inc.com/Design/Design-Tools/Ferrite-Core-Loss-Calculator>
- [3] [https://cdn.ozdisan.com/ETicaret\\_Dosya/652386\\_243124.pdf](https://cdn.ozdisan.com/ETicaret_Dosya/652386_243124.pdf)
- [4][https://cdn.ozdisan.com/ETicaret\\_Dosya/501245\\_5372110.pdf](https://cdn.ozdisan.com/ETicaret_Dosya/501245_5372110.pdf)
- [5] [https://cdn.ozdisan.com/ETicaret\\_Dosya/483083\\_5853486.pdf](https://cdn.ozdisan.com/ETicaret_Dosya/483083_5853486.pdf)
- [6] [https://cdn.ozdisan.com/ETicaret\\_Dosya/356189\\_1310147.pdf](https://cdn.ozdisan.com/ETicaret_Dosya/356189_1310147.pdf)
- [7] [https://cdn.ozdisan.com/ETicaret\\_Dosya/342170\\_703953.pdf](https://cdn.ozdisan.com/ETicaret_Dosya/342170_703953.pdf)